

Rapid Communications

The Rapid Communications section is intended for the accelerated publication of important new results. Manuscripts submitted to this section are given priority in handling in the editorial office and in production. A Rapid Communication may be no longer than 3½ printed pages and must be accompanied by an abstract and a keyword abstract. Page proofs are sent to authors, but, because of the rapid publication schedule, publication is not delayed for receipt of corrections unless requested by the author.

Alpha-clustering systematics from the quasifree ($p, p\alpha$) knockout reaction

T. A. Carey,* P. G. Roos, N. S. Chant, A. Nadasen, and H. L. Chen

Department of Physics and Astronomy, University of Maryland, College Park, Maryland 20742

(Received 19 August 1980)

Cross sections for the ($p, p\alpha$) reaction at 101.5 MeV have been measured for nine nuclei ranging from ^{16}O to ^{66}Zn . Distorted-wave impulse approximation analyses of the ground state transitions provide relative alpha-cluster spectroscopic factors in qualitative agreement with ($^6\text{Li}, d$) studies, although quantitative differences exist. The calculations are sensitive to the bound alpha-cluster parametrization, so that the experimental data suggest limits on the rms radius of the cluster-core wave function.

[NUCLEAR REACTIONS $^{16}\text{O}, ^{20}\text{Ne}, ^{24}\text{Mg}, ^{28}\text{Si}, ^{32}\text{S}, ^{40}\text{Ca}, ^{48}\text{Ti}, ^{54}\text{Fe}, ^{66}\text{Zn} (p, p\alpha)$,
 $E = 101.5$ MeV; Measured ($E_p, E_\alpha, \theta_p, \theta_\alpha$); DWIA analysis; deduced spectroscopic factors.]

Distorted-wave Born approximation (DWBA) analyses of ($^6\text{Li}, d$) cross section measurements on even-even nuclei in the $2s-1d$ and $1f-2p$ shells by Anantaraman *et al.*¹ show an interesting oscillatory structure in the extracted alpha-cluster spectroscopic factors, peaking near the closed shell nuclei ^{16}O and ^{40}Ca and rising for the $f-p$ shell nuclei. A different DWBA analysis of the same data² is in excellent agreement with those reported in Ref. 1 for $44 \leq A \leq 52$, but yields values for $52 \leq A \leq 66$ which remain small and relatively constant. However, an analysis by Hanson *et al.*³ of ($^6\text{Li}, d$) data obtained at about the same energy tends to support the original conclusions of Ref. 1. These analyses differ principally in their choices of optical model potentials for the DWBA calculations. Thus, there appears to be considerable sensitivity to the choice of these potentials as might be expected since the ($^6\text{Li}, d$) reaction is poorly momentum matched for $L = 0$ transitions (typically by more than 200 MeV/c at 0° for the energies used).

As an alternative, alpha cluster spectroscopic factors can be determined using quasifree alpha knockout reactions which have the advantage that momentum matching is possible at any bombarding energy. Studies of the ($p, p\alpha$) reaction at 100 MeV

on $1p$ -shell nuclei⁴ provide absolute spectroscopic factors in good agreement with shell model predictions. Tests of the reaction mechanism^{4,5} indicate that the distorted-wave impulse approximation⁶ (DWIA) provides a satisfactory description of the ($p, p\alpha$) reaction at these energies. Furthermore, the proton and alpha optical potentials required for the distorted wave analysis are certainly better known than the ^6Li potentials needed for the equivalent ($^6\text{Li}, d$) analysis. We therefore chose to measure the ($p, p\alpha$) reaction for nine of the nuclei studied with the ($^6\text{Li}, d$) reaction, to explore the oscillatory structure observed in Ref. 1.

The experiment was carried out using a 101.5 MeV proton beam from the University of Maryland Cyclotron to bombard solid targets of ^{24}Mg (>99%), ^{28}Si (natural SiO_2), ^{40}Ca (natural), ^{48}Ti (>99%), and ^{66}Zn (>99%) and gas targets of ^{16}O (natural), ^{20}Ne (>99%), and ^{32}S (natural H_2S). The outgoing protons were detected with a 4.2 msr solid state detector telescope consisting of a 500 μm Si surface barrier ΔE and a 15 mm intrinsic Ge E detector. The outgoing alpha particles were detected in a 1.3 msr 200 $\mu\text{m}/4$ mm Si solid state $\Delta E/E$ detector telescope.⁷ Overall, the absolute error due to target thicknesses,

Faraday cup, solid angles, uncertainties in dead time corrections, etc., was less than 10%.

For each target an energy sharing distribution (cross section as a function of detected proton energy) was obtained at a single quasifree coplanar angle pair. The proton telescope was fixed at $\theta_p = 70^\circ$, and the alpha telescope set on the opposite side of the beam at an angle such that zero recoil momentum of the residual nucleus in its ground state was kinematically allowed. The angles ranged from $\theta_\alpha = -44.9^\circ$ to -46.3° depending on the ground state Q value. A binding energy spectrum, obtained by summing the proton, alpha, and residual nucleus kinetic energies, is shown for $^{40}\text{Ca}(p, p\alpha)$ in Fig. 1. These data show the ground, 2^+ (2.2 MeV), and 4^+ (4.4 MeV) states in ^{36}Ar clearly resolved. Extracted energy sharing distributions for the ^{36}Ar ground state data, as well as those for $^{16}\text{O}(p, p\alpha)^{12}\text{C}$ (g.s.) and $^{66}\text{Zn}(p, p\alpha)^{62}\text{Ni}$ (g.s.), are shown in Fig. 2. Results for the other targets are similar.

The theoretical analysis of these data was carried out using the DWIA code of Chant,⁶ in which the three-body cross section for $(p, p\alpha)$ is written as

$$\frac{d^3\sigma}{d\Omega_p d\Omega_\alpha dE_p} = F_K S_\alpha \left. \frac{d\sigma}{d\Omega} \right|_{p-\alpha} \sum_A |T_L^A|^2, \quad (1)$$

where F_K is a known kinematic factor, S_α is the alpha-cluster spectroscopic factor, $(d\sigma/d\Omega)|_{p-\alpha}$ is a two-body half off-shell cross section for $p-\alpha$ scattering, and T_L^A is an amplitude involving incident and emitted particle distorted waves and a bound alpha-core wave function. We have chosen to approximate $(d\sigma/d\Omega)|_{p-\alpha}$ by the two-body on-shell cross section corresponding to the final

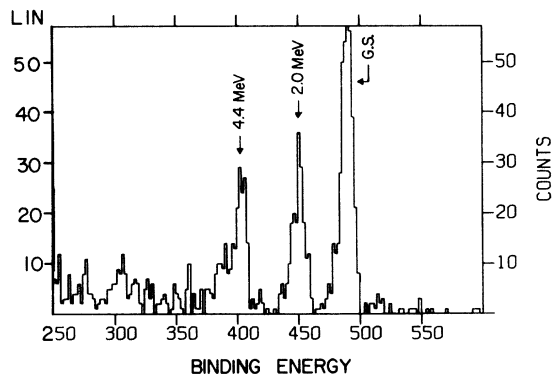


FIG. 1. Binding energy spectrum for $^{40}\text{Ca}(p, p\alpha)^{36}\text{Ar}$.

state of the outgoing $p-\alpha$ system (final energy prescription). This approximation should cause no difficulty since off-shell effects have been shown to be small⁴ for the typical binding energies involved. Furthermore, the use of a fixed proton angle for all targets leads to only a $\pm 4\%$ variation in the on-shell two-body cross section at the peaks of the energy sharing distributions. Thus, relative spectroscopic factors should be largely unaffected by the choice of prescription for $(d\sigma/d\Omega)|_{p-\alpha}$.

Since it was our primary goal to obtain systematic results for relative alpha-cluster spectroscopic factors, optical model potentials for the distorted waves were chosen in which target mass and incident energy dependence was treated in a systematic fashion. The proton potentials were taken from the work of Nadasen *et al.*,⁸ who obtained a global potential by fitting proton elastic scattering data for four targets at energies ran-

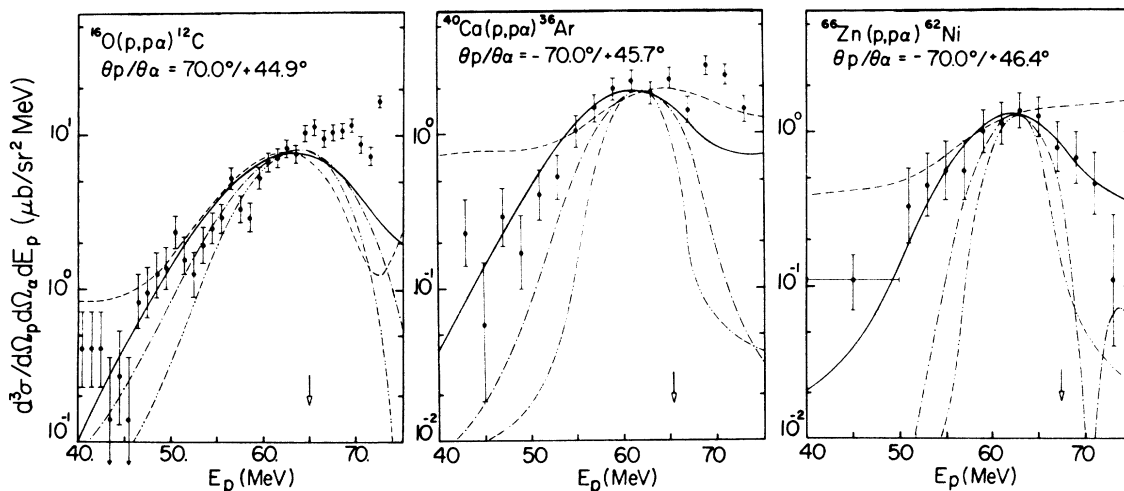


FIG. 2. Energy sharing distributions for $(p, p\alpha)$ ground state transitions. Curves are normalized DWIA calculations for different alpha particle bound state radius parameters r_0 (0.7, ----; 1.3, —; 1.9, -.-.-; 2.5, -.-.-).

ging from 40 to 180 MeV. No spin-orbit potentials were included in the DWIA calculations. Alpha potentials were obtained from the compilation of Perey and Perey.⁹ Parameters were chosen on the basis of a smooth mass and energy dependence of the volume integrals and rms radii for a wide range of nuclei, including higher energy results with unique Woods-Saxon potentials.

As is customary in alpha-transfer analyses the bound cluster wave function was calculated in a Woods-Saxon well, the depth of which was chosen to reproduce the ground state separation energy. The principal quantum number was chosen on the basis of conservation of oscillator quanta; i.e., 3S for $^{16}\text{O} \rightarrow ^{12}\text{C}(\text{g.s.})$, 5S for $^{40}\text{Ca} \rightarrow ^{36}\text{Ar}(\text{g.s.})$, and 7S for $^{66}\text{Zn} \rightarrow ^{62}\text{Ni}(\text{g.s.})$. The shape parameters were taken to be those used by Anantaraman *et al.*¹ ($r_0 = 1.3$ fm, $a = 0.65$ fm, where $R = r_0 A^{1/3}$ and A is the residual mass) in order to facilitate comparison with their results.

The results of DWIA calculations are shown in Fig. 2 for the ^{16}O , ^{40}Ca , and ^{66}Zn targets. The arrow on each abscissa indicates the location of the zero recoil momentum point ($p_3 = 0$). The normalization of the calculations was chosen to provide a best fit to the measured distribution, excluding regions to the right of the $p_3 = 0$ point (higher T_p), which appear to be contaminated by contributions from sequential inelastic scattering processes of the type $p + A \rightarrow p' + A^*$, where $A^* \rightarrow B + \alpha$. Such processes are clearly evident in ^{16}O and ^{40}Ca , but we believe them to be negligible below $T_p \approx 65$ MeV, which corresponds to excitation energies in the target nucleus in excess of about 30 MeV.

The value of $r_0 = 1.3$ fm used by Anantaraman *et al.* provides a satisfactory fit to all of the experimental data. We have therefore used this value to extract S_α to be compared with previous results. The spectroscopic factors plotted as a function of target mass for these, as well as $^{12}\text{C}(p, p\alpha)^8\text{Be}$ data obtained previously,⁴ are presented in Fig. 3 along with the results of Ref. 1. The errors are dominated by statistics, but include relative errors such as target thickness uncertainties. It is clear that our $(p, p\alpha)$ relative spectroscopic factors generally support the $(^6\text{Li}, d)$ work of Ref. 1, although suggesting a somewhat smaller rise in S_α in the $1f-2p$ shell.

It is interesting to note that the calculated absolute $(p, p\alpha)$ cross section is particularly sensitive to the bound state radius parameter, changing by approximately a factor of 2 for a 0.1 fm variation of r_0 . Shown in Fig. 2 are calculations for other values of the bound state radius normalized at $p_3 = 0$. We see that, unlike alpha transfer reactions, the shape of the calculated energy

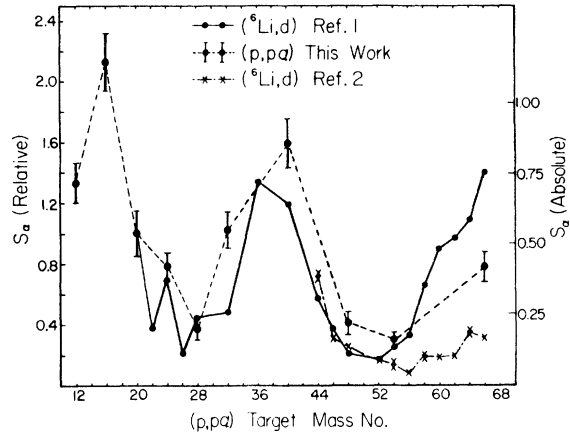


FIG. 3. Extracted spectroscopic factors for ground state transitions as a function of target mass. The lines merely guide the eye. The left scale indicates the relative value (normalized to unity at $A = 20$) and the right scale the absolute value extracted in $(p, p\alpha)$.

sharing distributions is sensitive to the bound state radius parameter, particularly for the heavier nuclei. Thus the data provide limits on the acceptable range of r_0 values ($r_0 \approx 1.2 - 1.6$ fm for heavier nuclei). This sensitivity to r_0 is expected to be enhanced as the bombarding energy is increased.¹⁰ Note that large values of r_0 (≥ 1.9 fm) are totally unacceptable. Such large radius parameters have been used in the past for $(\alpha, 2\alpha)$ reactions¹¹ and various transfer reactions^{12,13} [often obscured by writing $R = r_0 (A^{1/3} + 4^{1/3})$] in order to obtain absolute spectroscopic factors in agreement with shell model predictions. The present result suggests either a need for additional reaction mechanisms in these calculations or that alpha clustering differs as a function of the radial region probed in the reaction.

A systematic variation in r_0 with target mass will also change the general slope of the extracted S_α . Without theoretical guidance or higher energy $(p, p\alpha)$ data to provide more stringent limits on the value of r_0 , we cannot further define the variation in S_α with target mass. However, this will not remove the oscillatory behavior.

Various changes in the distorting potentials lead to relatively little change in shape, thereby preserving the sensitivity of the reaction to r_0 , but change the magnitude by up to 30%. However, these variations again do not change the conclusions concerning the general oscillatory behavior of S_α . The peaks in S_α occur at or near doubly magic nuclei where $2p-2h$ or $4p-4h$ components (which are included neither in the present analysis nor those of Refs. 1-3) may be quite important. These components lead to higher

principal quantum numbers and thereby an increased yield even with a small admixture.

The absolute values of S_α extracted in $(p, p\alpha)$ are also indicated in Fig. 3. These tend to be higher than calculated shell model¹⁴ or SU(3) (Ref. 15) values; for example, shell model calculations¹⁴ yield $S_\alpha[{}^{20}\text{Ne} - {}^{16}\text{O}(\text{g.s.})] = 0.18$. We expect the uncertainty in the extracted value of S_α to be no more than $\pm 50\%$ due to the optical model potential and off-shell uncertainties. However, changes in the bound state parametrization can produce much larger variations. For example, the consistent use of $r_0 = 1.4$ fm would reduce all S_α by roughly a factor of 2 in better agreement with the shell model predictions. Again without an improved theoretical treatment of the nuclear

clustering problem or more sensitive data, one cannot attribute the larger values for S_α for the lighter nuclei to increased clustering beyond that contained in conventional shell model calculations. However, it is quite clear that the $2s-1d$ shell model calculations or a simple SU(3) scheme are inadequate for the nuclei toward the upper end of the $2s-1d$ shell.¹⁶

This work has been supported in part by the National Science Foundation. The authors would like to thank the staff at the Maryland Cyclotron for their help in all phases of this work. The support of the University of Maryland Computer Science Center for the DWIA calculations is gratefully acknowledged.

*Present address: P Division, Los Alamos Scientific Laboratory, Los Alamos, New Mexico.

¹N. Anantaraman *et al.*, Phys. Rev. Lett. **35**, 1131 (1975).

²H. W. Fulbright *et al.*, Nucl. Phys. **A284**, 329 (1977).

³D. L. Hanson *et al.*, in *Clustering Aspects of Nuclear Structure and Nuclear Reactions (Winnipeg, 1978)*, Proceedings of the Third International Conference on Clustering Aspects of Nuclear Structure and Nuclear Reactions, edited by W. T. H. van Oers, J. P. Svenne, J. S. C. McKee, and W. R. Falk (AIP, New York, 1978), p. 716.

⁴P. G. Roos *et al.*, Phys. Rev. C **15**, 69 (1977).

⁵A. A. Cowley *et al.*, Phys. Rev. C **15**, 1650 (1977).

⁶N. S. Chant and P. G. Roos, Phys. Rev. C **15**, 57 (1977).

⁷T. A. Carey, Ph.D. thesis, University of Maryland, 1979 (unpublished).

⁸A. Nadasen *et al.*, Phys. Rev. C **22**, 1394 (1980).

⁹C. M. Perey and F. G. Perey, *Atomic Data and Nuclear Data Tables* (Academic, New York, 1976), Vol. 17,

No. 1.

¹⁰N. S. Chant, in *Clustering Aspects of Nuclear Structure and Nuclear Reactions (Winnipeg, 1978)*, Proceedings of the Third International Conference on Clustering Aspects of Nuclear Structure and Nuclear Reactions, edited by W. T. H. van Oers, J. P. Svenne, J. S. C. McKee, and W. R. Falk (AIP, New York, 1978), p. 415.

¹¹C. W. Wang *et al.*, Phys. Rev. C **21**, 1705 (1980).

¹²G. J. Wozniak, D. P. Stahel, J. Cerney, and N. A. Jolley, Phys. Rev. C **14**, 815 (1976).

¹³H. Yoshida, Phys. Lett. **47B**, 411 (1973).

¹⁴For example, W. Chung *et al.*, Phys. Lett. **79B**, 381 (1978).

¹⁵For example, J. P. Drayer, Nucl. Phys. **A237**, 157 (1975).

¹⁶For example, the shell model calculations of Ref. 14 give S_α of 0.18 for ${}^{20}\text{Ne}$ and 0.043 for ${}^{40}\text{Ca}$ compared to our experimentally measured values which indicate a value for ${}^{40}\text{Ca}$ larger than that for ${}^{20}\text{Ne}$.